Energy Calculations for Isotactic Polypropylene: A Contribution To Clarify the β Crystalline Structure

Dino R. Ferro,*,† Stefano V. Meille,‡ and Sergio Brückner§

Istituto di Chimica delle Macromolecole del CNR, Via E. Bassini 15, I-20133 Milano, Italy, Dipartimento di Chimica, Politecnico di Milano, Via Mancinelli 7, I-20131 Milano, Italy, and Dipartimento di Scienze e Tecnologie Chimiche, Università di Udine, Via del Cotonificio 108, I-33100 Udine, Italy

Received March 24, 1998; Revised Manuscript Received July 13, 1998

ABSTRACT: An analysis of the crystal structure of the β polymorph of isotactic polypropylene (β-iPP) is carried out with the methods of molecular mechanics, taking into account simultaneously intra- and intermolecular interactions. Results indicate that efficient crystal packing may be achieved in a number of different, nearly isoenergetic arrangements, most of them showing the features of frustration. This fact may well be due to the low density of β-iPP as compared to its other crystalline polymorphs. The most stable β-iPP structure is found in space group $P3_1$. *Up−down* disordering modes, found also in α- and γ-iPP, have marginally higher energy and give rise to $P3_121$ symmetry, without superposition of methyl groups belonging to anticlined chains. This structure, involving random *up−down* disordering, is thus proposed as the best average structure for individual β-iPP domains. Mechanisms for twinning among different domains are also investigated in order to explain the observed hexagonal symmetry of electron diffraction patterns.

Introduction

In a previous article, hereafter referred to as paper **I**, Meille et al.[1] proposed a novel crystal model for the β phase of isotactic polypropylene (β-iPP), based on X-ray and electron diffraction data analyses and supported by preliminary packing energy calculations. Here we present a detailed report on the progress of the packing energy calculations with the aim of further clarifying the complex problems posed by the β phase of iPP. Other models,[2,3] similar although different with regard to several relevant details, were developed independently and at about the same time as paper **I**. The differences between the more relevant of the proposed structures will also be discussed in the present paper.

The methodology utilized here is based on the simultaneous optimization of intra- and intermolecular interactions and is the same already applied with some success to tackle several structural problems concerning polymeric crystalline materials.[4−7] A similar approach was also devised by Boyd and co-workers.[8,9] An elegant presentation of the method was later published by Rutledge and Suter.[10] Our previous work showed that molecular mechanics can be fruitfully coupled with standard crystallographic techniques for various purposes: (i) to refine experimental models so that both crystallographic and stereochemical requirements are fulfilled;[4−7] (ii) to evaluate the effect of packing forces on the chain conformation;[5] (iii) to provide a priori models to be subsequently tested by crystallographic procedures, when the quality of the experimental data is too poor;[6] (iv) to evaluate and rationalize the relative stability of different polymorphs.[5−7] With regard to the last point, in the three cases examined (α/γ poly(pivalolactone),[5] α/β isotactic 1,4-*cis*-poly(2-methyl-1,3-pentadiene),[6] and α/γ iPP[7]), the calculations yielded molecular structures showing small energy differences between the two phases being compared, in semiquantitative agreement with the available thermodynamical data. Finally, in the study of the α and γ phases of iPP also the role of statistical disorder involving *up−down* chain orientation could be discussed. The above results suggest that our approach and the force-field utilized are well suited for a thorough analysis of the "hexagonal" phase of iPP.[11] This problem is complicated by the fact that the β-form is the iPP polymorph with the highest degree of disorder, as is made apparent by the diffuse scattering streaks characterizing its electron diffraction patterns[3,1] and as is also consistent with its relatively low density.

Method of Calculation

The present study consists of an exhaustive search of the energy minima for various structural models of β-iPP. For each space group considered, the total potential energy, defined as the sum of bonded and nonbonded intramolecular interactions and of nonbonded intermolecular interactions, is minimized with respect to all the atomic Cartesian coordinates of the asymmetric unit, the unit cell dimensions being kept unchanged. Thus each refined model corresponds to the lowest energy minimum for a given symmetry. In some cases additional relevant minima are identified.

The force field adopted is Allinger's MM2,[12] whose parameters for hydrocarbons have been established and tested for many years and which we utilized in our previous studies on crystalline polymers.[4−7] In the present investigation we removed the only minor difference with respect to the original MM2 potential, concerning the computation of the torsional term, which now is represented by one independent term for each dihedral angle. Moreover, while the intermolecular energy was previously computed as the sum of interactions between whole monomeric units, up to a cutoff distance of 8 Å, here we adopted a single interatomic cutoff distance of 11 Å: this allows for the elimination of quite small energy differences (of the order of a few hundredths of kilocalories per mole) arising when chains running in opposite directions at a given site are chosen as the reference. Repetition of previous energy minimizations on α- and γ-iPP proved that,

† Istituto di Chimica delle Macromolecole del CNR.
‡ Politecnico di Milano.
§ Università di Udine.

S0024-9297(98)00459-8 CCC: $15.00
Published on Web 09/12/1998

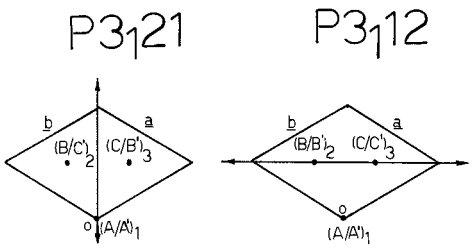

Figure 1. Comparison of space groups $P3_121$ and $P3_112$ showing the different orientations of the 2-fold axes relative to the cell. The three positions (1, 2, and 3) of the iPP helices are also shown.

besides eliminating inconsistencies, such changes have negligible effects on the relative stabilities of the various polymorphs. Other details concerning the method of calculation, including the treatment of up/down chain statistical disorder, can be found in the previous articles.[4−7]

All computations were carried out with the system CHAMP/93,[13] which is the latest version of the molecular mechanics program developed in this laboratory. A feature of the program particularly useful for the present work is that the input is structured as a series of commands, controlled by a simple but effective meta-language which allows for automatic repetition of previous commands with a wide possibility of changing parameters and files. This feature made a systematic search of the lowest energy structures possible with little manual effort. As a consequence, each identified minimum is the result of several independent energy minimizations, leaving very little margin to uncertainty (on the order of 0.01 kcal/mol) for the calculated relative stability of the different structures. In all calculations the lattice dimensions were kept constant at values corresponding to the experimental three-chain trigonal unit cell having $a = b = 11.02$ and $c = 6.49$ Å[11,1] (cell A in Figure 1 of paper **I**). Energies (expressed in kilocalories per mole) are always referred to three monomer units.

Results

Space Group $P3_121$ vs $P3_112$. Crystallographic indications[1] based on the observed electron diffraction intensities suggest that trigonal or hexagonal space groups with $p3$ or $p6$ projections are unlikely and that models characterized by centrosymmetric projections or by projection symmetry $p3m1$ are less plausible than models with projection symmetry $p31m$. With these considerations in mind, we initially set forth to determine the lowest-energy structural models in space groups $P3_121$ and $P3_112$. In a preliminary calculation, the intramolecular energy of the isolated helix was minimized also imposing the 3_1 symmetry and the experimental axial advancement per monomer unit $h = c/3 = 2.163$ Å. The resulting helix, properly roto-translated, was usually the starting point of the lattice calculations. Given the considerable rigidity of the iPP chain, we note that the results can hardly depend on the details of the initial conformational model.

As shown in Figure 1, space groups $P3_121$ and $P3_112$ present a common unit cell (cell A in Figure 1 of paper **I**), but differ for the orientation of the 2-fold axes with respect to the lattice axes. The unit cell contains six right-handed helices, each with occupancy 0.5, located at the three sites indicated as 1 at ($x = 0$, $y = 0$), 2 at ($x = {}^2/_3$, $y = {}^1/_3$), and 3 at ($x = {}^1/_3$, $y = {}^2/_3$). Three chains (labeled A, B, and C) are independent while the other three (A′, B′, and C′) are symmetry related by the 2-fold axes orthogonal to the helix direction. Primed and unprimed chains have therefore opposite directionalities; i.e., if unprimed chains are *up*, primed are *down*. In $P3_112$ the three sites are independent and interchangeable, i.e., we have A and A′ at site 1 and B and B′ at site 2 while C and C′ are at 3. This arrangement which we represent as $(A/A')_1$, $(B/B')_2$, and $(C/C')_3$ differs from the one in $P3_121$ which displays nonequivalent sites. At site 1 in the latter space group there are two coexisting symmetry-related helices so that we have $(A/A')_1$, whereas at both sites 2 and 3 the two statistically copresent *up* and *down* helices are not symmetry related; i.e., we have a situation that can be represented as $(B/C')_2$ and $(C/B')_3$. Site 1 differs thus by symmetry from sites 2 and 3 and locating one chain at 1 and one (or two) independent chains at 2, we give rise to an example of *frustrated structure*[14] as implied in ref 1 and explicitly proposed in ref 3. While $P3_112$ requires completely random up/down statistical disorder, i.e., 0.5 occupancy factors, and no correlation between neighboring sites, $P3_121$ may be consistent with occupancy factors other than 0.5 (e.g. 1) at sites 2 and 3.

As in previous related investigations,[5,7] we did not rely on any existing model to determine the most stable structure. A first search of what proved to be the lowest-energy $P3_121$ structure was carried out in steps as follows: in each of two different runs two independent chains were considered, assuming partial disorder by combining helices $(A/A')_1$ at the origin either with helices $(B)_2$ and $(B')_3$ or with $(C')_2$ and $(C)_3$. In each case, a grid of 4×13 starting points for minimization was selected by fixing one methyl carbon of helix A on the 2-fold axis and by roto-translating helix B (or C) about its axis in steps of 30° and ${}^1/_{12}$ of c, so that an angle of 120° and a whole c unit were spanned. Similar runs were repeated with only one chain also at position 1, i.e., with no disorder at all. The best results of such energy minimizations were then combined in final runs with three independent chains: the most stable structure found is shown in Figure 2a, while the corresponding fractionary atomic coordinates are given in Table 1. Although the above search might appear insufficient, since it did not initially take into consideration B···C and C′···B′ correlations between sites 2 and 3 before the final stage of full energy minimization, no lower point was ever found in later searches.

In a similar way, we proceeded to determine the most stable $P3_112$ models. This space group presents considerably less freedom, since the methyl groups of all three *up*/*down* symmetry-related helix pairs are forced to lie close to the 2-fold axes. The initial model was built by rotating the $(A/A')_1$ pair of the lowest-energy $P3_121$ model by 90° about the c axis and placing parallel pairs of helices also at sites 2 and 3; a second starting point was obtained from the former one by roto-translating only the helices at the origin by 180° and $c/2$; in models of this kind the methyl carbons were located at $z = 0$. Grids of 64 starting points were then obtained from the previous ones by combining roto-translations of the three independent chains by ±20° and ±0.5 Å or by 0°, 180° and 0, $c/2$. In practice, energy minimization yields only two acceptable $P3_112$ structures: the most stable one (minimum I, shown in Figure 2b) has a total energy higher than $P3_121$ by only 0.24 kcal/mol of trimer, while minimum II is definitely less stable (0.84 kcal/mol above $P3_121$). To compare the packing efficiency of the above β models with that of the structures previously computed for the α and γ phases of iPP, the lowest energy minima corresponding to space groups $C2/c$ and $Fddd$ were recomputed with the present force-field version:

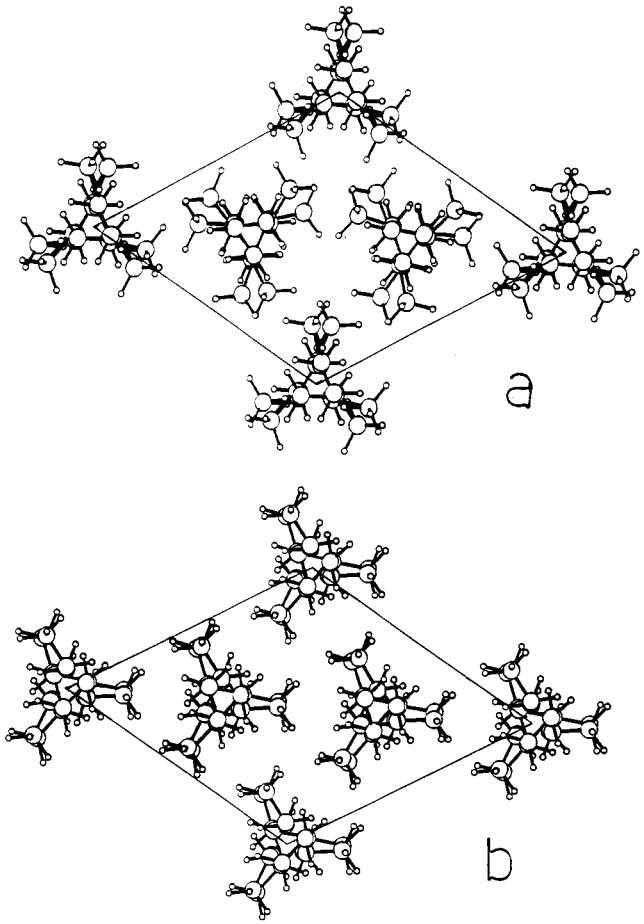

Figure 2. The most stable structures computed in space group $P3_121$ (a) and $P3_112$ (b).

the results are summarized in Table 2, while Table 3 describes the β models in terms of polar coordinates of the methyl carbons of the three independent 3_1 helices. In Figure 3 we give a definition of rotations ϕ_z and traslations t_z used to specify the positions of the three chains in the cell. These polar coordinates are sufficient when chains obey a rigorous 3_1 symmetry (trigonal or hexagonal space groups) but give only an approximate description in other (e.g. orthorhombic) space groups.

The results discussed so far (see Table 3) are in reasonable agreement with independent crystallographic findings:[1] in fact the $P3_121$ model is slightly but significantly more stable than the $P3_112$ structure, which in turn presents a higher disagreement factor R considering both X-ray and electron diffraction data. Moreover, against the experimental diffraction evidence, the latter model collapses into the one-chain trigonal subcell, as the three independent chains are in essence identical, while $P3_121$ presents three distinct helices. Thus, interestingly, the less stable $P3_112$ model is not frustrated, contrary to recent morphological evidence,[14] whereas the $P3_121$ model is frustrated. It is also not surprising that the best model of the metastable, less dense β phase has a higher energy (by only 0.3 kcal/mol) than the similarly disordered α-iPP model. A related remarkable feature of the $P3_121$ model, which is clearly visible in Figure 2a and in Table 3, is the lack of rigorous isosterism between *up* and *down* coexisting helices; thus the symmetry-related methyl carbons of the pair $(A/A')_1$ do not superpose, but form an angle Δ_z of 20° and are displaced along c by $\Delta t_z = 0.83$ Å. Even higher deviations affect the pair of independent helices

Table 1. Atomic Fractional Coordinates Corresponding to the Lowest Energy $P3_121$ Model[a]

	x	y	z
	Chain A		
C2	0.0096	0.0737	−1.0744
H21	0.0679	0.1819	−1.1389
H22	−0.1017	0.0291	−1.1226
C1	0.0122	0.0831	−0.8373
H1	0.1238	0.1323	−0.7878
C3	−0.0411	0.1822	−0.7694
H31	0.0151	0.2850	−0.8506
H32	−0.1550	0.1355	−0.8021
H33	−0.0246	0.2065	−0.6019
	Chain B		
C2	0.4101	0.7264	−1.2238
H21	0.5174	0.7673	−1.2880
H22	0.3747	0.8007	−1.2723
C1	0.4190	0.7327	−0.9865
H1	0.4595	0.6628	−0.9362
C3	0.5276	0.8825	−0.9189
H31	0.6300	0.9196	−0.9979
H32	0.4910	0.9579	−0.9548
H33	0.5499	0.8887	−0.7509
	Chain C		
C2	0.6731	0.2668	−0.5865
H21	0.6334	0.1595	−0.6505
H22	0.7846	0.3306	−0.6351
C1	0.6727	0.2591	−0.3492
H1	0.5621	0.1906	−0.2989
C3	0.7548	0.1866	−0.2807
H31	0.7158	0.0841	−0.3600
H32	0.8685	0.2531	−0.3151
H33	0.7435	0.1635	−0.1127

[a] Helix B is centered at $(^1/_3\ ^2/_3)$, helix C at $(^2/_3\ ^1/_3)$, in the trigonal reference system. The three *down* helices A′, B′, and C′ are generated by the 2-fold axis $a + b$.

Table 2. Relative Stabilities of the iPP Polymorphs, Computed with the MM2 Force Field

	with up/down disorder		without up/down disorder	
phase	space group	ΔE (kcal/mol)	space group	ΔE (kcal/mol)
α	*C*2/*c*	0.00	*Cc*	−0.41
			$P2_1/c$	−0.50
γ	*Fddd*	−0.11	*Fd*2*d*	−0.55
			*F*2*dd*	−0.54
β	$P3_121$	0.29	$P3_1$	0.005
	$P3_121$ (4 chains)	0.09		
	$P3_112$	0.53	$P3_1$ (subcell)	0.29

$(B/C')_2$ at site 2 (and by symmetry the $(C/B')_3$ pair at site 3): the *up* chain is roto-translated by $\Delta_z = 27°$ and $\Delta t_z = 0.87$ Å with respect to the anticlined helix. We shall return to this point when comparing the present $P3_121$ model with the one proposed by Lotz and coworkers.[3]

Effect of Up/Down Disorder on Packing Energy. As in the study of the α and γ phases,[7] we investigated the energetic cost of up/down chain statistical disorder by partially or totally removing the statistical coexistence of anticlined helices at sites 1, 2, and 3. Partial removal of up/down disorder is achieved, for example, in the already mentioned four-chain $P3_121$ symmetry system $(A/A')_1$, $(B)_2$, $(B')_3$, with two independent chains. This system still contains up/down disorder at the origin, so the occupancy is 0.5 and 1.0 for A and B chains, respectively. Total removal of up/down disorder is achieved in systems with one independent chain at each of the three sites 1, 2, and 3. In this case symmetry is lowered from $P3_112$ (or $P3_121$) to $P3_1$. In general, energy minimizations starting from the minimum of Figure 2a, after removal of disorder at sites 2 and 3 or

Table 3. Description of the Lowest-Energy $P3_121$ and $P3_112$[a] Models of β-iPP

space group	min no.	E_{tot} (kcal/mol)		helix A ϕ_{z1} (deg)	helix A t_{z1} (Å)	E_A (kcal/mol)	helix B ϕ_{z2} (deg)	helix B t_{z2} (Å)	E_B (kcal/mol)	helix C ϕ_{z3} (deg)	helix C t_{z3} (Å)	E_C (kcal/mol)
$P3_121$	I	−2.69	*up*	10.0	−0.67	−3.14	−54.8	−1.64	−2.57	−38.2	−1.82	−2.37
			down	−10.0	−1.50		−81.8	−2.51		−65.2	−2.69	
$P3_112$	I	−2.45	*up*	87.9	0.30	−2.45	87.6	0.28	−2.45	87.9	0.30	−2.45
			down	92.1	−0.30		92.4	−0.28		92.1	−0.30	
$P3_112$	II	−1.85	*up*	81.4	−0.05	−2.94	90.3	0.39	−1.07	128.2	0.95	−1.53
			down	98.6	0.05		89.7	−0.39		51.8	−0.95	

[a] For this space group, the reference system was chosen so that the 2-fold axis normal to the *a* axis passes through the origin.

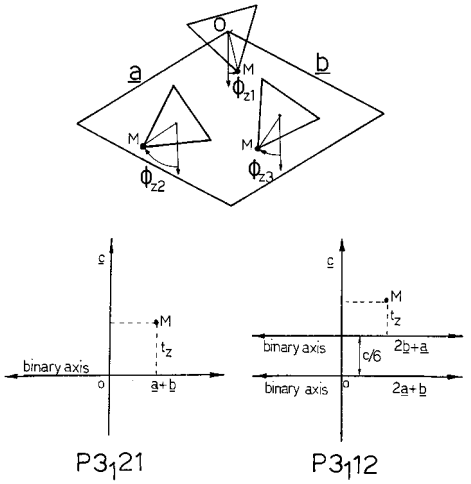

Figure 3. Rotations ϕ_z and translations t_z relative to the unit cell geometry for space groups $P3_121$ and $P3_112$.

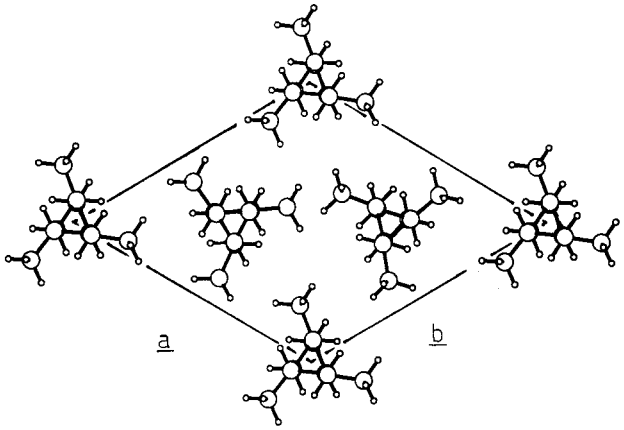

Figure 4. The most stable UUD structure in $P3_1$ symmetry.

at all three sites, led to models for which the structure of the independent units is rather close to the starting one. Thus, we obtained two basic nonequivalent $P3_1$ models, which may be labeled according to the chain orientations (U = up; D = down) at sites 1, 2, and 3 respectively, namely (UUD) and (UUU). A little thought should convince the reader that these are the only nonequivalent combinations since in $P3_1$ the three sites are equivalent and only the relative orientations of the three independent chains matter: (UDD) is therefore equivalent to (UUD), (DUU), (DDU), etc. In Figure 4 we show one of the (UUD) models optimized in the $P3_1$ symmetry. We found in this way several nearly isoenergetic $P3_1$ symmetry minima, all of them frustrated, but the possibility that other even lower minima had been missed was also considered. To ensure that the model found is indeed the lowest energy $P3_121$ structure and to obtain the complete list of low energy structures corresponding to various degrees of disorder, an additional search was performed. Again, the fully disordered six-chain $P3_121$ structure was first considered: a grid of $6 \times 10 \times 3^3$ points was generated by translating chain B in steps of *c*/6, by translating chain C in steps of *c*/10, and by rotating all three chains by ±20° and 0°. To save computer time all such points were minimized with a low cutoff distance and the more promising minima were selected for full minimization. Another wider grid of $5^2 \times 4^3$ points was built by combining B and C translations by *c*/5 and rotations of the three chains by 30°: low cutoff minimization led to 49 distinct minima, which reduced to 37 after full minimization; of these minima, only 12 proved nonequivalent by symmetry. The lowest energy structures are described in Table 4.

The coordinates of the above 37 minima were then also used as starting points of several calculations with a lower degree of disorder. Thus, due to the redundancy of the initial models, the results, summarized in Table 4, offer a rather complete picture of the preferred $P3_1$-21 and $P3_1$ arrangements of iPP. As one can see in Tables 3 and 4, the effect of lowering the degree of disorder and symmetry has modest effects on packing energy and on the geometry of the most stable arrangements, somewhat smaller than the effects already computed for α- and γ-iPP.[7] This means that in the lowest-energy completely disordered minimum (I) all combinations of chain···chain interactions are nearly optimal, so that removal of disorder releases only about 0.1 kcal/mol of trimer per site, with adjustments of a few degrees in ϕ_z and translations of about 0.1 Å. The analysis of energy contributions shows that site 1 is significantly more stable than 2 and 3, owing to less favorable $(C)_3\cdots(C')_2$ and also $(C)_3\cdots(B)_2$ interactions. There are several nearly isoenergetic $P3_1$ arrangements with anticlined helices, mostly corresponding to different choices of three-chain combinations from the six-chain $P3_121$ minimum I, while there is just one model with isoclined (UUU) helices having energy only slightly higher than the absolute $P3_1$ minimum and coordinates quite close to those pertaining to the $P3_121$ minimum. We finally observe that the nonfrustrated $P3_1$ (UUU) structure obtained from minimum I in $P3_112$, which reduces to the one-chain subcell, is again less stable by 0.3 kcal/mol than the minimum derived from the $P3_1$-21 symmetry, just as for the models with statistical up−down disorder.

Combining Helices of Opposite Chirality. In paper **I**, it was pointed out that tilted electron-diffraction patterns show a higher symmetry than expected for space group $P3_121$, and it was argued that this feature could be the result of additional crystallographic or

Table 4. Low-Energy Arrangements of iPP Helices in $P3_121$, $P3_1$, and $P6_122$ Crystals[a]

site occupancy 1	site occupancy 2	site occupancy 3		no. of indep chains	tot. energy (kcal/mol)	ϕ_{z1} (deg)	t_{z1} (Å)	ϕ_{z2} (deg)	t_{z2} (Å)	ϕ_{z3} (deg)	t_{z3} (Å)
					$P3_121$						
U/D	U/D	U/D		3							
			I		−2.69	10.0	−0.67	−54.8	−1.64	−38.2	−1.82
			II		−1.83	−2.2	−0.98	−51.8	−1.64	23.9	−0.64
			III		−1.76	9.1	−0.75	−53.3	−1.64	24.9	−0.64
			IV		−1.62	25.1	−0.31	−46.0	−1.72	20.7	−0.64
			V		−1.21	25.8	−0.37	11.0	−0.94	−37.8	−1.47
			VI		−0.66	7.7	−0.61	−41.8	1.62	−30.8	−1.67
					$P3_121$						
U/D	U	D		2							
			I		−2.90	7.0	−0.62	−54.0	−1.64	(54.0	−0.52)
			II		−2.59	12.0	−0.67	38.4	−0.33	(−38.4	−1.83)
			III		−1.84	−2.6	0.62	−49.0	1.57	(49.0	2.75)
			IV		−1.70	−1.7	−0.54	−47.2	1.64	(47.2	2.68)
			V		−1.29	15.1	1.58	49.7	−2.79	(−49.7	0.63)
			VI		−0.79	10.1	−0.97	31.3	−0.06	(−31.3	2.10)
					$P3_1$						
U	U	D		3							
			I		−2.98	11.5	−0.54	−61.0	−1.87	45.2	−0.76
			II		−2.79	−40.0	−1.67	4.9	−0.59	−35.8	−1.67
			III		−2.76	−44.2	−1.51	−32.2	−1.76	−16.7	−1.70
			IV		−2.70	21.3	0.56	39.6	0.75	2.1	−0.54
			V		−2.07	5.4	−0.54	−54.9	1.59	38.5	2.68
			VI		−0.78	10.5	−1.01	27.8	−0.09	−34.2	−2.17
					$P3_1$						
U	U	U		3							
			I		−2.92	8.1	−0.71	56.2	−1.57	−39.1	−1.87
			II		−2.11	9.8	−0.47	−57.3	1.39	−26.5	−1.58
					$P6_122$						
				2							
					−1.62	31.4	−0.13	−42.7	−1.72	17.3	−0.63

[a] In this table and in the following ones, at sites with vicariant chains the polar coordinates refer to the *up* helix.

twinning glide mirror planes. Such additional symmetry elements would imply the coexistence of helices of opposite chiralities within the same crystal or at least in adjacent twins. As shown in Figure 8 of paper **I**, the proposed structure of β-iPP can be described, utilizing the orthorhombic cell O, as a series of trilayers of chains, running normal to the orthorhombic *b* axis. While in $P3_121$ (and in $P3_1$ in the absence of up/down disorder) such trilayers, formed by chains of the same chirality, are simply translated one after the other, a glide plane generates trilayers of opposite chirality, and could give rise to space groups *P*2*nn* or *P*2*na*. We investigated the feasibility of such arrangements from the point of view of packing efficiency.

The 37 previous minima were again used to generate a sufficient number of trilayer arrangements, consistent with the given O cell (a = 11.03 Å, b = 19.08 Å, c = 6.49 Å) and with the mentioned space groups *P*2*nn* and *P*2*na*. Then the degree of disorder was lowered in all the distinct ways as previously done for $P3_121$. It was found that, while no space group presents acceptable arrangements when *up*/*down* disorder is imposed at all sites, the symmetry operation ($x + {}^1/_2$, $-y + {}^1/_2$, $z + {}^1/_2$) (*n*-glide plane normal to *b* in the O cell) yields a reasonable packing when setting only one helix at site 2, the anticlined one at site 3 and allowing for *up*/*down* statistics at site 1 (space group *P*2*nn*). An even lower minimum is obtained (see Table 5) by removing disorder also at site 1 (implying suppression of the binary axis parallel to *a*) and locating there a chain isoclined with that of site 2 and anticlined with that of site 3. In this case the space group symmetry reduces to *Pn* (monoclinic) even though cell O has all three angles equal to 90°. The lowest-energy structures arising from the above symmetry operation are listed in Table 5. We note that in these computations the rigorous 3_1 symmetry of a single chain is lost: preserving the 3-fold screw axis would raise the total energy by 0.1−0.2 kcal/mol. If the *P*2*nn* symmetry is applied to the fully disordered trilayer in the arrangement optimal for the $P3_121$ space group, the interactions between the $(B)_2$ and $(B')_3$ chains of opposite chirality across the glide mirror plane highly destabilize the structure, causing a large roto-translation of these chains. Vice versa the $(A/A')_1$ chains are only slightly affected, and chains $(C)_3$ and $(C')_2$ of opposite chirality interact moderately. Therefore, upon removal of the $(B)_2$ and $(B')_3$ chains, the remaining molecules can return to a position close to the optimal one: this situation was already depicted in Figure 8b of paper **I**. Hence such a symmetry operation is a conceivable mechanism for crystal microtwinning although not a very favored one, since even in the best considered cases energies higher than for the optimal $P3_121$ space group by ca. 0.5 kcal result.

Other Space Groups. The above idea was generalized to many other symmetry operations, always applied to the trilayers (at *b*/4) so as to pack them efficiently in the O cell. Symmetry elements were first coupled with a binary axis parallel to *a* in order to generate *up*/*down* disorder and then they were applied only to selected triples of isoclined or anticlined chains so that space group symmetries as low as triclinic $P\bar{1}$ could arise (only one center of inversion present) even though the metrically orthorhombic cell (cell O) was adopted. The results of these computations, summarized in Table 6, confirm that $P3_121$ is the only space group capable of packing the fully disordered trilayers with only three crystallographically independent chemical repeats. The number of other symmetry elements that can be applied to specifically oriented chain arrangements producing an

Table 5. Low-Energy Arrangements of iPP Helices in *P*2*nn* and Lower Symmetry Crystals[a]

site occupancy				no. of indep chains	tot. energy (kcal/mol)	ϕ_{z1} (deg)	t_{z1} (Å)	ϕ_{z2} (deg)	t_{z2} (Å)	ϕ_{z3} (deg)	t_{z3} (Å)
1	2	3									
					*P*2*nn*						
U/D	U/D	U/D		3							
			I		−1.17	16.6	−0.63	−89.7	−2.46	−34.3	−1.61
			II		+1.92	−1.4	−0.85	−51.7	1.76	−29.1	−1.40
					*P*2*nn*						
U/D	D	U		2							
			I		−2.16	15.7	−0.60			−34.6	−1.66
U/D	U	D		2							
			II		−0.39	18.6	−0.63	−89.1	−2.51		
					Pn						
U	U	D		3							
			I		−2.23	−44.1	−1.72	25.7	−0.59	−17.1	−1.49
			II		−1.75	−37.3	0.36	30.8	1.35	17.3	0.36
			III		−1.59	25.3	−0.67	−2.6	0.13	−32.6	−1.69
			IV		−1.48	54.5	−0.15	2.1	−0.90	−25.3	−1.55
			V		−1.42	33.4	1.30	−37.8	−0.23	−39.2	−0.63
					Pn						
U	U	U		3							
			I		−1.71	−37.7	−1.39	25.5	−0.34	−31.8	−1.40
			II		−1.52	−27.9	−0.47	28.0	0.77	53.4	−1.46
			III		−1.28	−31.1	−0.51	32.6	0.20	21.3	−0.53
					Pn						
U	D	D		3							
			I		−1.72	−46.2	1.28	−11.8	1.61	20.3	2.25
			II		−1.58	−33.0	0.87	29.9	1.27	29.4	1.41
			III		−1.55	−34.9	0.96	48.4	2.96	−0.5	1.87
			IV		−1.30	−39.3	−0.42	48.9	1.34	−32.8	1.28

[a] Due to lack of perfect 3_1 symmetry, the description of these models is approximate.

acceptable packing is however impressive. Such arrangements may therefore contribute locally to the overall structure disorder. In particular, the symmetry operations $(-x + {}^1/_2, -y + {}^1/_2, z + {}^1/_2)$, i.e. a binary screw axis parallel to *c*, and $(-x + {}^1/_2, -y + {}^1/_2, z + {}^1/_2)$, i.e., an inversion center, yield structures as stable as the lowest energy $P3_1$ structures and containing respectively only isochiral and antichiral chains in neighboring trilayers.

Twinning modes based on trilayers perpendicular to the orthorhombic *b* axis may appear unlikely as they would give rise to streaks along the $1\bar{1}0$ and not along the 110 direction of the trigonal cell[3] (A in Figure 1 of paper **I**), as experimentally observed. However, considering the system symmetry, an appropriate combination with other symmetry elements allows us in fact to evaluate the energetics of a broad range of local arrangements, clearly implying that a number of low-energy twinning modes involving both isochiral and antichiral helices must exist. A complete analysis of all the energetically plausible disordering modes in β-iPP is beyond the scope of the paper, but the reader should be convinced by now that a broad range of possibilities exists.

As mentioned, hexagonal symmetry is suggested by tilted crystal electron diffraction intensities. It is clear that such higher symmetry implies higher levels of disorder, necessarily involving somewhat higher packing energies than for more ordered structures. Up to now we discussed attempts to achieve this symmetry essentially by occasional twinning, but hexagonal space groups with statistical disorder are also a possible, although not very promising, alternative to be considered. Two space groups appeared more likely, namely $P6_122$ and $P6_422$, both combining both the 2-fold axes orientations characterizing respectively $P3_121$ and $P3_1$-12 (Figure 1). They also present a 6-fold axis at site 1 whereas 3_1 axes are present at positions 2 and 3. We considered eight chains per unit cell, four at site 1 (occupancy 0.25) and two (anticlined) at each of the equivalent sites 2 and 3 (occupancy 0.5), only one chemical repeat at site 1, and one at site 2 being independent. Whereas space group $P6_422$ produces only high energy structures, starting from minimum I of $P3_1$-21 and adopting $P6_122$ symmetry, we obtained a model which, despite the high complexity and the reduced degrees of freedom, has a relatively low energy, ca. 1 kcal/mol higher than model I ($P3_121$). This model, which is also frustrated, is described in Table 4 in the same reference system as the other space groups and is not labeled being unique. One can see that chain A at site 1 has undergone a significant roto-translation and the *up* chain at site 3 has a completely different orientation with respect to the model computed in the $P3_121$ symmetry; the B chain, on the contrary, is close to its original position.

Comparison with Other Proposed Models. As we mentioned in the Introduction, Lotz and co-workers[3] proposed a model of β-iPP (hereafter labeled as the LKD structure) closely related to the structure presented in paper **I**. Although the two models share the same $P3_1$-21 space group, the detailed organization of the iPP helices presents significant differences, as one can see by comparing Figure 8a of paper **I** with Figure 4 of ref 3. The more apparent difference is that the methyl carbons of statistically disordered *up* and *down* helices in the LKD model show perfect superposition, which is lacking in the structure proposed in paper **I**. This rather surprising feature, which according to our analysis distinguishes β-iPP from the α and the γ polymorphs, is essential in order to obtain a good agreement between observed and calculated *hk*0 electron diffraction intensities (see paper **I**). Also, in the computed minimum-energy model, *up* helices are rotated counterclockwise

Table 6. Effects of Different Operators Acting on the Trilayer Structure Reported in Figure 8 of Paper I and Included, in the Same Figure, in Cell O (Orthorhombic)[a]

symmetry operation	space group	site occupancy 1	2	3	no. of indep chains	tot. energy (kcal/mol)	ϕ_{z1} (deg)	t_{z1} (Å)	ϕ_{z2} (deg)	t_{z2} (Å)	ϕ_{z3} (deg)	t_{z3} (Å)
$x + 1/2, y + 1/2, z$	$P3_121$											
		U/D	U/D	U/D	3	−2.69	10.0	−0.67	−54.8	−1.64	−38.2	−1.82
		U/D	U	D	2	−2.90	7.0	−0.62	−54.0	−1.64		
	$P3_1$											
lack of binary axis		U	U	D	3	−2.98	11.5	−0.54	−61.0	−1.87	45.2	−0.76
		U	U	U	3	−2.92	8.1	−0.71	56.2	−1.57	−39.1	−1.87
$x + 1/2, -y + 1/2, z + 1/2$	$P2nn$											
glide plane n + binary axis		U/D	U/D	U/D	3	−1.17	16.6	−0.63	30.3	−0.30	−34.3	−1.61
		U/D	D	U	2	−2.16	15.7	−0.60			−34.6	−1.66
$x + 1/2, -y + 1/2, z + 1/2$	Pn											
lack of binary axis		U	U	D	3	−2.23	−44.1	−1.72	25.7	−0.59	−17.1	−1.49
		U	D	D	3	−1.72	−46.2	1.28	20.3	2.25	−11.8	1.61
		U	U	U	3	−1.71	−37.7	−1.39	25.5	−0.34	−31.8	−1.40
$-x + 1/2, -y + 1/2, -z$	$P2/b$											
center of inv. + binary axis		U/D	U/D	U/D	3	−1.79	9.3	−0.73	−61.3	−1.81	−36.9	−1.68
$-x + 1/2, -y + 1/2, -z + 1/2$	$P\bar{1}$											
lack of binary axis		U	U	U	3	−2.93	−39.4	−0.71	10.3	0.52	−53.1	−0.27
		U	D	D	3	−2.92	12.5	0.45	50.8	0.46	−7.4	−0.66
		U	U	D	3	−2.74	−50.2	−0.51	41.5	0.63	0.9	−0.52
$-x + 1/2, -y + 1/2, z + 1/2$	$P222_1$											
binary screw axis + binary axis		U/D	U/D	U/D	3	−1.92	11.4	2.50	−49.8	1.57	−38.0	1.9
		U/D	U	D	2	−2.20	13.5	−0.63	8.1	−0.56		
$-x + 1/2, -y + 1/2, z + 1/2$	$P2_1$											
lack of binary axis		U	D	D	3	−3.05	12.7	2.88	51.1	2.80	−7.8	1.79
		U	U	U	3	−2.92	25.5	−0.63	1.8	−0.47	−53.8	−1.64
		U	U	D	3	−2.91	6.8	2.25	−49.3	1.01	−12.0	1.17
$-x + 1/2, -y + 1/2, z$	$P2$											
		U	D	D	3	−2.09	21.1	2.94	55.3	−0.30	−5.6	1.88
		U	U	U	3	−2.06	36.8	2.99	6.0	−0.20	−53.3	1.91
		U	U	D	3	−1.39	16.9	0.41	46.0	−2.70	−7.6	−0.60
$-x + 1/2, y + 1/2, -z + 1/2$	$P2_1$											
		U	U	D	3	−2.92	7.8	2.13	−53.3	1.10	49.3	2.13
		U	U	U	3	−2.90	9.9	2.05	−52.5	1.10	−37.9	0.82
		U	D	D	3	−2.77	−51.2	−2.24	−4.6	−2.06	−17.9	−1.83
$-x + 1/2, y + 1/2, -z + 1/2$	$P2_1$											
		U	U	D	3	−2.54	29.6	0.89	31.6	0.93	16.5	0.10
		U	U	U	3	−2.54	30.0	0.90	25.0	0.78	29.6	0.92
		U	D	D	3	−2.47	−30.5	−0.04	−19.9	−0.71	−20.6	−0.72
$-x + 1/2, y + 1/2, z$	Pb											
		U	U	D	3	−2.53	−46.1	1.54	17.5	2.48	−24.1	1.73
		U	U	U	3	−2.44	10.6	2.58	−57.9	1.67	37.2	1.65
		U	D	D	3	−2.07	−41.1	1.83	57.4	3.10	−57.7	1.40
$x + 1/2, y + 1/2, -z + 1/2$	Pn											
		U	D	D	3	−2.89	15.2	0.53	47.9	0.19	−2.4	−0.56
		U	U	U	3	−2.89	20.9	−2.78	6.0	−2.43	−52.1	2.71
		U	U	D	3	−2.75	−38.5	2.72	7.8	−2.61	−43.2	2.59

[a] The indicated space groups correspond to the hypothesis that the given elements of symmetry act systematically throughout the crystal. Monoclinic and triclinic space groups always refer to cell O, and therefore angles α, β, and γ are always equal to 90°.

by about 20° and translated along *c* by about 0.80 Å relative to *down* chains, thus producing a relevant displacement between methyl groups of anticlined helices. In the notation of Table 3, both chains A and A′ in the LKD structure have $\phi_z = 0°$ and $t_z = 1/6\ c$, and the chains at sites 2 and 3 are shifted exactly by $\pm 1/3c$. Moreover, while in the LKD structure chain $(B)_2$ is slightly displaced counterclockwise with respect to $(B')_3$, the position halfway between B and C′ in our model is rotated significantly in the opposite sense; in other words, chain $(B)_2$ has a very similar orientation in the two models, but $(C')_2$ in our model is rotated by −27°. Finally, in our model the average positions of the methyl carbons at the three different sites are relatively shifted by a value close to but not coincident with $\pm 1/3c$.

The LKD model thus appears in essence as a simplification of minimum I, and we decided to check whether the apparent complication of our model was not only crystallographically but also energetically justified. Therefore, we applied the constraints present in the LKD model to the $P3_121$ microcrystal (six chains in the unit cell with three independent chemical repeats), by properly fixing the coordinates ϕ_z and t_z of the methyl carbons. In a first run, the rotation of chain B was optimized imposing the constraint $\phi_{zB} = -\phi_{zC}$ and varying this parameter continuously around the position proposed in ref 3. The resulting optimized structure has a total energy of −0.77 kcal/mol, which is 1.92 kcal/mol of trimer higher than minimum I. Similar curves $E(\phi_{zB})$ were computed by releasing t_z's and/or ϕ_{zA} and ϕ_{zC}:

these runs showed that both the rotational and translational constraints contribute to the large excess energy in the LKD model, while limited concerted roto-translations can occur at little energy cost (perturbations of ϕ_{zB} of ±5° without constraints raises the total energy by only 0.1 kcal/mol). Analysis of the lattice energy contributions shows that chain C is the least stable one in the LKD model, owing to interactions of its methyl group with two methylenes belonging respectively to the A and C′ chains. This observation is important in our opinion because it indicates that packing *is not* dominated by methyl−methyl interactions and therefore superposition of methyls belonging to anticlined chains is unlikely to be a required feature of the structure.

As pointed out by Lotz et al.,[3] the model in ref 3 does not show short methyl···methyl contacts; hence the relatively large energy difference with respect to the lowest $P3_121$ minima, as well as with respect to the α and γ structures, as computed with Allinger's MM2 force field, is both surprising and puzzling. To make sure that such a result is not an MM2 artifact, we looked for supporting evidence in calculations based on an independently derived, all-atom force field. The intermolecular energy, which accounted for 1.62 kcal/mol of the total difference in the MM2 calculation, was computed for the two models, without minimization, using the nonbonded potentials of Biosym's CFF91 force-field.[15,16] The result indicates a difference of 1.41 kcal/mol, in good agreement with MM2. On the contrary, similar calculations carried out with Jorgensen's OPLS "united-atom" force field,[17] where CH_3, CH_2, and CH groups are treated as spheres, yield an intermolecular energy difference of −0.44 kcal/mol. Hence, in the latter case, the total energy would favor the LKD model by 0.14 kcal/mol. These results are only indicative, as all terms of each force field ought to be utilized together, in independent full minimizations. A thorough comparison of force fields is however beyond the scope of the present work while the ultimate criterion lies, of course, in the ability of a method to reproduce the available experimental data. In previous related investigations,[4,5] we already ascribed the ability of our approach to account for subtle conformational and packing effects just to the explicit inclusion of hydrogen atoms and to the usage of Allinger's potentials while avoiding unnecessary restrictions. Hence our experience, also supported by the result obtained with CFF91, induces us to rather rely on the "full-atom" treatments than on simplified ones, the more so if we consider that backbone CH and CH_2 groups are not free to rotate and that to represent them as spheres is therefore hardly satisfactory.

Comparison with the Crystallographic Model. The up−down disordered, stereochemically constrained structural model that gives the best agreement with ED and unoriented X-ray diffraction data (paper **I**, hereafter ED model) is obtained for the same space group but does not correspond to the minimum energy model developed in the present work (minimum I). Differences are important since the ED structure is 2.36 kcal/mol of trimer higher than minimum I, and after unrestrained minimization, it falls into minimum V of Table 4. On the other hand all of the simpler models obtained from the present calculations, even considering simple modes of disordering, give disagreement factors which are substantially worse than the one of the ED model (typically 0.30 as compared to ca. 0.20), both with electron diffraction and powder X-ray diffraction data.

Discussion

The fact that the crystallographic approach (paper **I**) and the energetic analysis do not at present appear to converge toward a unique structural model for β-iPP may be interpreted as a failure at finding the correct structure. We cannot exclude that this might be the case, but in view of the results reported in the present analysis, we consider it more likely that what is commonly labeled as β-iPP corresponds to a variety of different local structures all compatible with the same unit cell and characterized by small energy differences. In fact packing energy calculations suggest that the structure of β-iPP may well be extremely complex. The lower density, as compared to α-iPP and γ-iPP, allows for a great number of different, almost equienergetic structures. We have shown that not only is practically random *up*/*down* statistics energetically allowed but also that this may be accomplished, at least occasionally, through rotations around two different crystallographic directions as in hexagonal $P6_122$ symmetry.

Although the crystallographic and the energetic models do not coincide, it should be emphasized that they do share some very basic features. First of all packing in space group $P3_121$ is favored, and furthermore, in the best structural model obtained in this space group, there is lack of superposition of methyl groups belonging to anticlined helices, just like in the model refined on crystallographic data. On the contrary, in the model refined in the $P3_112$ space group (only 0.24 kcal/mol higher) the isosterism requirement for statistically copresent anticlined molecules applies (Figure 2b). It may be interesting to compare the $P3_121$ and the $P3_1$-12 symmetries. The symmetry operations of the $P3_121$ space group imply that the helix axis location of *up*/*down* symmetry related helices does not coincide for chains positioned at site 2 (and 3). While an *up* helix located at site 1 generates a *down* helix still at site 1, placing an *up* chain at site 2 generates a *down* chain at site 3. Thus locating one helix at site 1 (the origin) and one (or two) independent helices at site 2 (see Figures 1 and 2a), we generate a disordered but also *frustrated structure* like the one proposed in ref 3 and recently observed by Lotz and co-workers.[14] In the $P3_112$ symmetry, on the contrary, the helix axes of symmetry related *up*/*down* pairs coincide in all cases, i.e., *up* chains at sites 1, 2, and 3 respectively generate *down* molecules located at the same site (i.e. 1, 2, and 3). In this respect the $P3_112$ space group favors a situation which is more similar to the one present in α- and γ-iPP structures, and we again observe superposition of methyl groups. At the same time, frustration practically disappears since the three sites are in essence equivalent (see Table 3 and Figure 2b). Comparing parts a and b of Figure 2, it is apparent that in the fully disordered model I ($P3_121$ symmetry, Figure 2a) *anticlined chains statistically copresent at site 2 (or 3) are related* to one another *through a noncrystallographic binary axis* which is not bound to any exact orientation and height in the unit cell. This results in a greater freedom in the local crystal packing than is allowed by the crystallographic binary axes present in $P3_112$ symmetry. We ascribe to this greater freedom the lowering in the crystal energy and the relevant deviations from methyl−methyl superposition of anticlined chains. The

basic condition for this freedom to be fully taken advantage of is of course the low density of the β-iPP polymorph, which makes the role of side methyl groups less critical for packing requirements. From this comparative analysis between the $P3_121$ and $P3_112$ space groups, we may conclude that frustration and the absence of superposition of methyl groups are related in origin. A further indication is that in this low-density β-modification, it is no longer sufficient to consider only repulsive methyl−methyl contacts in order to assert the feasibility of a structure. In particular it may be incorrect to *maximize* methyl−methyl distances since this may increase energy instead of reducing it. The $P3_121$ space group is, of course, the simplest *average* representation of the β-iPP structure with *up*/*down* disorder, while locally, in the absence of disorder, the $P3_1$ symmetry produces the lowest energy minimum with the (UUD) configuration or some of its proper permutations. The (UUU) configuration is however only 0.06 kcal/mol higher. Since the $P3_112$ arrangement involves only a small energy increase, we cannot exclude that local domains with this symmetry coexist with prevalent $P3_121$ ones: the features of possible boundary regions between these two structures are yet to be investigated.

Noticeably, the ordered minimum-energy model and all the models within 0.2 kcal/mol of trimer above the minimum are frustrated. This is not surprising, as the concept of frustration in crystal structure analysis of polymers means that in the unit cell different helices exist that are not symmetry related, i.e., each one adapts to the environment to achieve the minimum-energy arrangement. In this sense frustration is a special case of a broader tendency to give rise to asymmetric units comprising more than one molecule (or one monomer) in low-temperature crystal structures in order to minimize the internal energy of the crystal. Interestingly, whereas in β-iPP monomer units of a given helix are symmetry related and different helices may be independent, in the α- and γ-iPP structures monomer units within a given helix are crystallographically independent, and in fact, two quite different local environments can be recognized. The equivalence postulate between monomer units[18] in many cases represents a first-order approximation and should be taken just as a useful tool and not as a dogma.

As expected, we have not found any really satisfactory model in hexagonal symmetry, and this is again in agreement with results of crystallographic analysis that always give poor disagreement factors when this symmetry is adopted. The deepest minimum is found in $P6_122$ symmetry and is 1.07 kcal/mol higher than minimum I in $P3_121$ symmetry. In our opinion the experimental evidence supporting hexagonal symmetry in the diffraction patterns cannot be connected with any regularly repeating hexagonal structure. It is rather the result of frequent twinning between different crystal domains, each one with trigonal symmetry. Some of the twinning modes that have been examined (see Table 6) allow for inversion of helical chirality. This is surely sound since the $P3_121$, $P3_112$, $P3_1$, and $P6_122$ space groups require only isochiral helices and domains of helices of opposite chirality must necessarily exist.

As observed by Lotz et al., in view of the orientation along the 110 direction of the streaks observed in the (hk0) electron diffraction patterns, it is more likely that twinning would occur across the (110) plane than across the (200) plane. While in the previous paper **I** we only considered the latter hypothesis, we have now investigated both modes. Both orientations show some acceptable arrangements (see Table 6) so that it is difficult to propose an exclusive, simple coupling mode of different domains.

References and Notes

(1) Meille, S. V.; Ferro, D. R.; Brückner, S.; Lovinger, A. J.; Padden, F. J. *Macromolecules* **1994**, *27*, 2615.
(2) An, B. *Acta Polym. Sin.* **1993**, *3*, 330.
(3) Lotz, B.; Kopp, S.; Dorset, D. *C. R. Acad. Sci. Paris, Ser. IIb* **1994**, *319*, 187.
(4) Ferro, D. R.; Brückner, S. *Macromolecules* **1989**, *22*, 2359.
(5) Ferro, D. R.; Brückner, S.; Meille, S. V.; Ragazzi, M. *Macromolecules* **1990**, *23*, 1676.
(6) Ferro, D. R.; Brückner, S.;. Meille, S. V.; Ragazzi, M. *Macromolecules* **1991**, *24*, 1156.
(7) Ferro, D. R.; Brückner, S.;. Meille, S. V.; Ragazzi, M. *Macromolecules* **1992**, *25*, 5231.
(8) Sorensen, R. A.; Liau, W. B.; Boyd, R. H. *Macromolecules* **1988**, *21*, 194.
(9) Sorensen, R. A.; Liau, W. B.; Kesner, L.; Boyd, R. H. *Macromolecules* **1988**, *21*, 200.
(10) Rutledge, G. C.; Suter, U. W. *Macromolecules* **1991**, *24*, 1921.
(11) Keith, H. D.; Padden, F. J.; Kissel, W. J.; Wyckoff, H. W. *J. Appl. Phys.* **1959**, *30*, 1485.
(12) Allinger, N.; Yuh, Y. H. *QCPE*, **1980**, *12*, 395.
(13) Ferro, D. R.; Ragazzi, M. *Conformational (Hyper) Analysis Milan Package*; Istituto di Chimica delle Macromolecole del CNR: Milano, Italy, 1993.
(14) Stocker, W.; Schumacher, M.; Graff, S.; Thierry, A.; Wittmann, J.-C.; Lotz, B. *Macromolecules* **1998**, *31*, 807.
(15) *Biosym's CFF91 Force Field*; Biosym Technologies Inc.: San Diego, CA, 1991.
(16) Maple, J.; Dinur, U.; Hagler, A. T. *Proc. Natl. Acad. Sci. U.S.A.* **1988**, *85*, 5350.
(17) Jorgensen, W. L.; Tirado-Rives, J. *J. Am. Chem. Soc.* **1988**, *110*, 1657.
(18) Corradini, P. In *The Stereochemistry of Macromolecules*; Ketley, A. D., Ed.; Marcel Dekker: New York, 1968; Vol. 3, p 1.

MA9804592